

# BIFURCATING SOLUTIONS IN A NON-HOMOGENEOUS BOUNDARY VALUE PROBLEM FOR A NONLINEAR PENDULUM EQUATION.

FERNANDO P. DA COSTA, MICHAEL GRINFELD, JOÃO T. PINTO,  
AND KEDTYSACK XAYXANADASY

ABSTRACT. Motivated by recent studies of bifurcations in liquid crystals cells [1, 2] we consider a nonlinear pendulum ordinary differential equation in the bounded interval  $(-L, L)$  with non-homogeneous mixed boundary conditions (Dirichlet at one end of the interval, Neumann at the other) and study the bifurcation diagram of its solutions having as bifurcation parameter the size of the interval,  $2L$ , and using techniques from phase space analysis, time maps, and asymptotic estimation of integrals, complemented by appropriate numerical evidence.

## 1. INTRODUCTION

Motivated by the study of the twist-Fréedericksz transition in a nematic liquid crystal cell, a non-homogeneous Dirichlet boundary value problem for the nonlinear pendulum equation

$$(1) \quad x''(t) + \sin 2x(t) = 0,$$

for  $t$  in the interval  $[-L, L]$ , was considered in recent papers [1, 2], and the structure of the bifurcating solutions when the parameter  $L$  is changed was studied.

In this paper we consider again the existence of solutions for a non-homogeneous boundary value problem for equation (1), this time with a Dirichlet condition at  $t = -L$  and a Neumann one at  $t = L$ , a case that may be relevant for modelling the twist-Fréedericksz transition in a cholesteric liquid crystal cell [4]. The problem that will be considered is the following, illustrated in Figure 1,

$$(2) \quad \begin{cases} x' = y \\ y' = -\sin 2x, \end{cases}$$

$$(3) \quad x(-L) = -\phi, \quad y(L) = \phi^*.$$

where  $\phi^* := \sqrt{1 - \cos 2\phi}$ . System (2) has a first integral given by

$$(4) \quad V(x, y) = y^2 - \cos 2x.$$

and from  $V(-\phi, 0) = V(0, \phi^*)$  we conclude that the points  $(-\phi, 0)$  and  $(0, \phi^*)$  lie on the same orbit of (2), as illustrated in Figure 1 by the orbit denoted by  $\gamma^*$ .

---

*Date:* July 29, 2019.

*2010 Mathematics Subject Classification.* Primary 34B15, 34C23; Secondary 41A60.

*Key words and phrases.* Non-homogeneous two-points boundary value problems; Bifurcations; Nonlinear pendulum; Asymptotic evaluation of integrals.

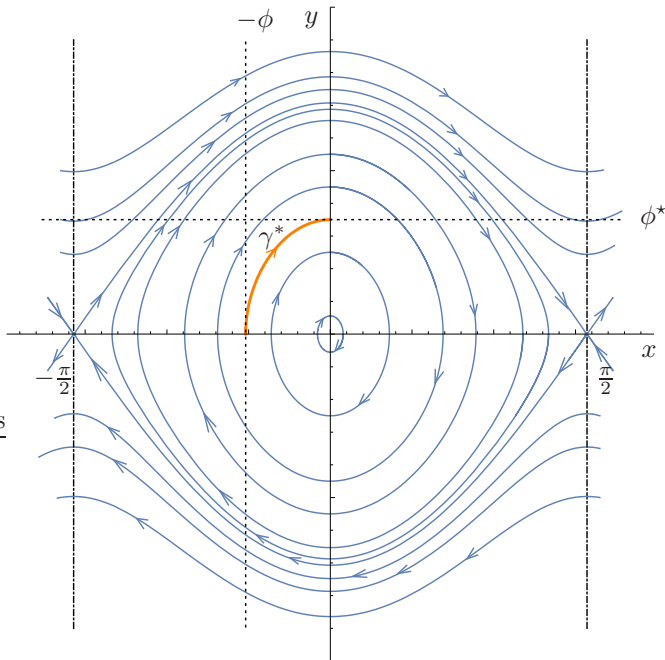


FIGURE 1. Phase plot of the orbits of equation (2), the boundary conditions (3) to be considered, and the orbit  $\gamma^*$  referred to in the text. The straight lines  $x = -\frac{\pi}{2}$  and  $x = \frac{\pi}{2}$  are to be identified.

This relation between the conditions imposed at the two boundary points entails a certain symmetry in the allowed solutions, akin to what happened in the case of Dirichlet boundary conditions studied in [1], and is a reasonable first step towards the understanding of the general case.

The tools used in this paper are based on appropriately defined time maps, measuring the time spent by a given orbit between two of its points. According to what will be most appropriate for the computations, we will identify an orbit by the ordinate of its first intersection either with the  $x$ -axis, the  $y$ -axis, or the line  $x = -\phi$ , leading to different, although equivalent, time maps.

We study the bifurcation diagram of solutions to (2)–(3) using the following procedure: we start by identifying a segment of an orbit of (2),  $\gamma^*$ , such that the corresponding solution, in addition to satisfying the boundary conditions (3),  $x(-L) = -\phi$  and  $y(L) = \phi^*$ , also satisfies  $y(-L) = 0$  and  $x(L) = 0$  (see Figure 1). We call the solution corresponding to  $\gamma^*$  a *critical solution* (and  $\gamma^*$  a *critical (segment of an) orbit*). Calling this solution *critical* is justified as we will prove that in bifurcation diagrams parameterized by  $L$ , there is more than one solution branch passing through it. To this (segment of) orbit  $\gamma^*$  corresponds a *critical time*  $T^*$ , and a corresponding critical value of  $L = L^* = T^*/2 > 0$ .

We then perturb this (segment of) orbit and investigate how the time spent changes relative to  $T^*$ . This time is measured by adequately defined time maps, whose definition arises naturally from the phase portrait and the first integral (4)

(see, e.g. [3, 6]). This approach was used in [1, 2] for the study of (2) with non-homogeneous Dirichlet boundary conditions; its application in the present case led to some unexpected difficulties and the analytical study had to be completed with numerical simulations providing solid evidence for a conjecture about the existence of a single minimum of the time maps of some solution branches.

## 2. TIME MAPS: DEFINITION AND BASIC RESULTS

For every  $\alpha \in (0, \frac{\pi}{2})$ , the orbit  $\gamma_\alpha$  of (2) that intersects the  $x$ -axis at  $(-\alpha, 0)$  is periodic. Using (2) and the first integral (4) the time taken from the point of intersection of  $\gamma_\alpha$  with the negative- $x$  semi-axis,  $(-\alpha, 0)$ , to the first intersection with the positive- $y$  semi-axis, occurring at the point  $(0, \sqrt{2} \sin \alpha)$ , is given by the following time map

$$(5) \quad T(\alpha) := \int_0^\alpha \frac{1}{\sqrt{\cos 2x - \cos 2\alpha}} dx.$$

We will also need to measure the time taken by  $\gamma_\alpha$  described above between its point of intersection with the positive- $y$  semi-axis,  $(0, \sqrt{2} \sin \alpha)$ , and the point of its first intersection with the vertical line  $x = \nu$ , with  $\nu \in (0, \frac{\pi}{2})$ . In the same way as above, the fact that (4) is a first integral allows us to conclude that this time is given by the time map

$$(6) \quad T_1(\alpha, \nu) := \int_0^\nu \frac{1}{\sqrt{\cos 2x - \cos 2\alpha}} dx.$$

Observe that  $T_1(\phi, \phi) = T(\phi)$ .

The proof of the following result can be consulted in [1].

**Proposition 1.** *Let  $0 < \phi < \alpha < \frac{\pi}{2}$ . The time maps  $T$  and  $T_1$  defined by (5) and (6), respectively, satisfy:*

- (1)  $\alpha \mapsto T(\alpha)$  is strictly increasing, and converges to  $+\infty$  as  $\alpha \rightarrow \frac{\pi}{2}$  and to  $\frac{\pi}{2\sqrt{2}}$  as  $\alpha \rightarrow 0$ .
- (2)  $\alpha \mapsto T_1(\alpha, \phi)$  is strictly decreasing.

To study the orbits located above the homoclinic orbit to  $(\frac{\pi}{2}, 0) \equiv (-\frac{\pi}{2}, 0)$  in the positive- $y$  semi-plane we use as an identifying parameter its intersection with some positive line (instead of the parameter  $\alpha$  above that in these cases is nonexistent, since these orbits do not intersect the  $x$ -axis). In [1, 2] the parameter used in these cases was the ordinate  $\beta$  of the intersection of the orbit with the positive- $y$  semi-axis. Here we shall use as parameter the value  $z = y(-L)^2$ , i.e., the square of the intersection of the orbit with the vertical line  $x = -\phi$ , or, in terms of the original boundary value problem, the square of the value of the derivative of the solution  $x(t)$  at the boundary point  $t = -L$ . For orbits intersecting the  $x$ -axis we can easily relate the parameters  $\alpha$  and  $z$  using the first integral (4):  $V(-\alpha, 0) = V(-\phi, \sqrt{z})$ . In order not to overload the notation we shall use the same symbols,  $T$  or  $T_1$ , for the time maps independently of which variable,  $\alpha$  or  $z$ , is being used in the parametrization of the orbits.

3. PHASE SPACE ANALYSIS OF ORBITS BIFURCATING FROM  $\gamma^*$ 

Let  $\gamma^*$  be the orbit of (2)–(3) shown in Figure 1. Let  $T^* = 2L^*$  be the time taken by this orbit. This orbit rests on the periodic orbit of (2) intersecting the negative  $x$ -axis at  $x = -\phi$ . Slightly perturbing this supporting periodic orbit to another whose intersection with the negative  $x$ -axis is at  $-\alpha < -\phi$ , with  $\alpha - \phi$  sufficiently small, we easily conclude from the phase portrait and from the continuous dependence of solutions of ODEs on the initial data over finite time intervals, that there exists four distinct orbits satisfying (2)–(3) for appropriately chosen values of  $L$  close to  $L^*$ . We shall denote these as solutions of type  $I$ ,  $A$ ,  $B$ , and  $C$ , as illustrated in Figure 2.

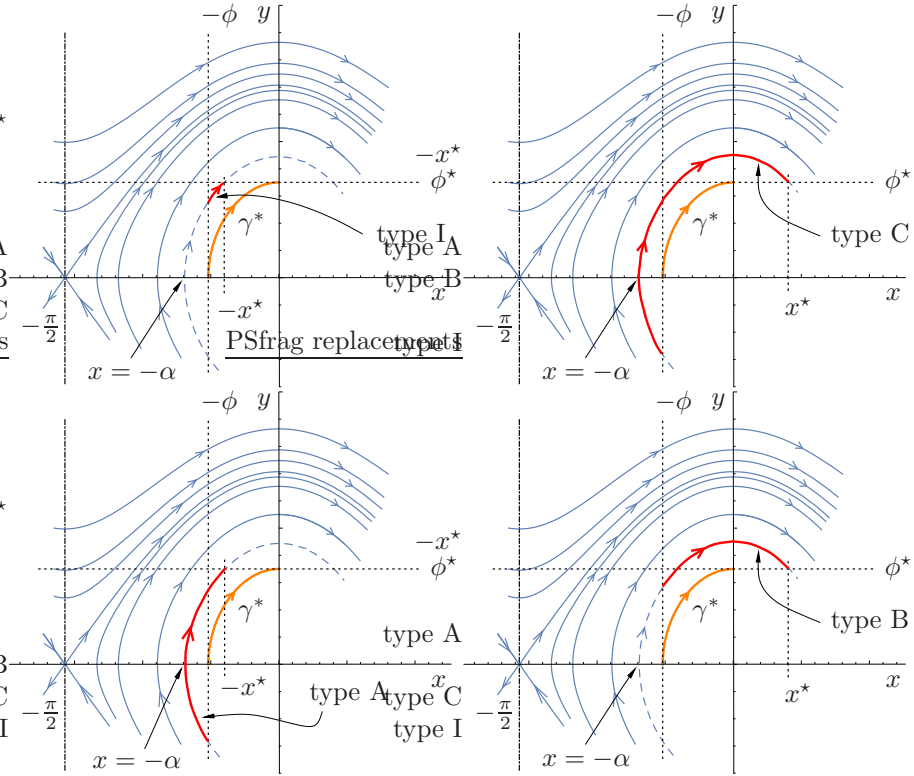


FIGURE 2. Phase space illustration of the four types of orbits of (2)–(3) obtained by a perturbation of the orbit  $\gamma^*$ , denoted by  $A$ ,  $B$ ,  $C$ , and  $I$ .

Taking into account the time maps defined in Section 2 the time spent in each orbit of the above types is given by, respectively,

$$(7) \quad T_I(\alpha, \phi) := T_1(\alpha, \phi) - T_1(\alpha, x^*)$$

$$(8) \quad T_A(\alpha, \phi) := 2T(\alpha) - (T_1(\alpha, \phi) + T_1(\alpha, x^*))$$

$$(9) \quad T_B(\alpha, \phi) := T_1(\alpha, \phi) + T_1(\alpha, x^*)$$

$$(10) \quad T_C(\alpha, \phi) := 2T(\alpha) - (T_1(\alpha, \phi) - T_1(\alpha, x^*))$$

where  $x^*$  is the positive solution of  $V(x^*, \phi^*) = V(-\alpha, 0)$ , i.e.,

$$(11) \quad x^* = x^*(\alpha, \phi) := \frac{1}{2} \arccos(1 - \cos 2\phi + \cos 2\alpha).$$

From the phase portraits in figures 1 and 2 we conclude that orbits of type *A* and *C* can be continued down to  $-\alpha \downarrow -\frac{\pi}{2}$ , which corresponds to their initial point converging to points on the homoclinic orbit to  $(-\frac{\pi}{2}, 0) \equiv (\frac{\pi}{2}, 0)$  in  $\{y < 0\}$ , but not further down: if the initial point gets to, or below, this homoclinic orbit the corresponding orbit remains in  $\{y < 0\}$ , and the solution will not satisfy the boundary condition  $y(L) = \phi^* > 0$ , for any value of  $L$ .

In contradistinction with these cases, in principle there is no obstruction to orbits of types *I* and *B* to be continued above the homoclinic orbit to  $(-\frac{\pi}{2}, 0) \equiv (\frac{\pi}{2}, 0)$  in  $\{y > 0\}$ . To properly handle this possibility it is convenient to parameterize the orbits, and the corresponding time maps, not by  $\alpha$  but by either the ordinate of its intersection with the positive  $y$ -axis,  $\beta$ , or by the ordinate of its initial point  $y(-L)$ , or, as we shall use in Section 4.4, by the square of this quantity  $z := y(-L)^2$ . Using these parameterizations the variable  $\alpha$  in the function  $x^*$  needs to be correspondingly changed to  $\beta$ ,  $y(-L)$ , or  $z$ , which is easily done using the fact that  $V$  is a first integral to relate the various parameters,  $V(-\alpha, 0) = V(0, \beta) = V(-\phi, y(-L)) = V(-\phi, \sqrt{z})$ , leading to the corresponding expressions for  $x^*$ . One that we shall frequently use in what follows is the expression in terms of  $z$ :

$$(12) \quad \bar{x}^*(z) := \frac{1}{2} \arccos(1 - z).$$

Notwithstanding the possibility of these orbits to be continued above the homoclinic, they cannot be continued for arbitrarily large values of  $y(-L)$ , although for different reasons, as we shall see below.

Type *I* orbits obviously cease to exist when  $y(-L) = \phi^*$ , since, when this occurs, the initial and final points of the orbit coincide (see Figure 3.) The reason why these

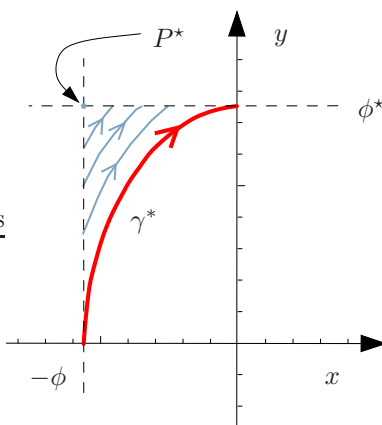


FIGURE 3. Continuation of type *I* orbits of (2)–(3) for the initial point of the orbit with increasing values of  $y(-L)$ , showing that, when  $y(-L) \rightarrow \phi^*$ , these orbits converge to a single point  $P^* = (-\phi, \phi^*)$  and then vanish.

orbits cannot be continued above this value of  $y(-L)$  is easy to understand from the phase portrait: since the initial and final points of type  $I$  orbits are always regular points of the phase plane, having  $y(-L)$  approaching the limit value  $\phi^*$  we have type  $I$  orbits taking less and less time  $2L$ , with  $L \rightarrow 0$  as  $y(-L) \rightarrow \phi^*$ , and thus (2)–(3) having no sense in the limit. In fact, analysis of the time maps tell us exactly the same: taking  $z \rightarrow (\phi^*)^2$  in (7) (with the variable  $z$  instead of  $\alpha$ ) and noting that, by (12) and the definition of  $\phi^*$ ,  $\lim_{z \rightarrow (\phi^*)^2} \bar{x}^*(z) = \phi$ , it immediately follows that  $T_I(z) \rightarrow 0$ . In section 4.1 a study of the monotonicity of  $T_I$  will be presented.

The situation for type  $B$  orbits is more interesting. Since all orbits of (2) above the orbit homoclinic to  $(-\frac{\pi}{2}, 0) \equiv (\frac{\pi}{2}, 0)$  in  $\{y > 0\}$  have an absolute minimum at  $x = \frac{\pi}{2}$ , there are no type  $B$  orbits resting on an orbit of (2) if the  $y$ -component of that minimum is bigger than  $\phi^*$ , since in this case no segment of the orbit (and in particular the one we call type  $B$  orbit) can satisfy the boundary condition  $y(L) = \phi^*$ . Using the first integral  $V$  this means that the largest value of  $y(-L)$  that a type  $B$  orbit must satisfy is given by  $V(-\phi, y(-L)) = V(\frac{\pi}{2}, \phi^*)$ , and so, from  $\phi^* = \sqrt{1 - \cos 2\phi}$ , we must have  $y(-L) = \sqrt{2}$ , independently of  $\phi$ . This implies that orbits of type  $B$  only exist for  $y(-L) \in (0, \sqrt{2}]$ .

To understand what is going on in this case we observe that, due to the periodicity of the vector field, for initial points  $(-\phi, y(-L))$  with  $y(-L)$  bigger than the ordinate of the point on the homoclinic orbit (but less than  $\sqrt{2}$ ), there is another orbit with end point  $(-x^*, \phi^*)$ . This orbit is part of a new class of orbits we shall call type  $B'$ . See Figure 4. When  $y(-L) \rightarrow \sqrt{2}$  the two end points of orbits of

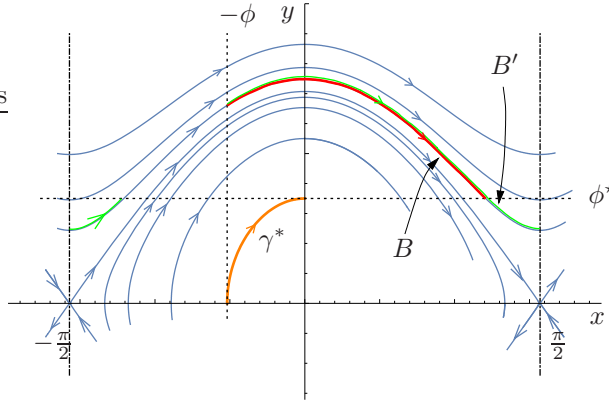


FIGURE 4. An orbit of (2)–(3) of type  $B$  above the homoclinic orbit and the orbit of type  $B'$  with the same  $y(-L)$ .

types  $B$  and  $B'$  converge to one another and at  $y(-L) = \sqrt{2}$  the two coincide with the point  $(\frac{\pi}{2}, \phi^*)$ , and both cease to exist for  $y(-L) > \sqrt{2}$ .

#### 4. BIFURCATION DIAGRAM OF ORBITS BIFURCATING FROM $\gamma^*$

To draw the bifurcation diagram of orbits bifurcating from  $\gamma^*$  we need to put together the information in Section 3, gathered from the phase portrait, with information about the time spent by each orbit, obtained from the study of the time maps, which we will do next.

**4.1. Behavior of type  $I$  solutions branch.** We first consider solutions of type  $I$ . From 7, the definition of the time maps (5) and (6), and Proposition 1, we conclude that

$$T_I(\alpha, \phi) = T_1(\alpha, \phi) - T_1(\alpha, x^*) < T_1(\alpha, \phi) < T_1(\phi, \phi) = T(\phi) = T^* = 2L^*.$$

Thus, in the bifurcation diagram plotted using the time spent by the orbit as the bifurcation parameter, type  $I$  branch of solutions exist to the left of the bifurcation point  $T^*$  correspondent to the critical orbit  $\gamma^*$ . Let us compute the derivative  $\partial T_I / \partial \alpha$ . From

$$\begin{aligned} \frac{\partial T_I}{\partial \alpha}(\alpha, \phi) &= \frac{\partial T_1}{\partial \alpha}(\alpha, \phi) - \frac{\partial T_1}{\partial \alpha}(\alpha, x^*) - \frac{\partial T_1}{\partial x^*} \frac{dx^*}{d\alpha} \\ &= - \int_{x^*(\alpha)}^{\phi} \frac{\sin 2\alpha}{(\cos 2x - \cos 2\phi)^{\frac{3}{2}}} dx \\ &\quad - \frac{2 \sin 2\alpha}{\sqrt{\cos 2x^*(\alpha) - \cos 2\phi} \sqrt{1 - (1 - \cos 2\phi - \cos 2\alpha)^2}}, \end{aligned}$$

we conclude that  $\partial T_I / \partial \alpha < 0$ , since it is clear from the definition of type  $I$  solutions that we always have  $x^* < \phi$  (see Figure 3). This means that the branch of type  $I$  solutions in the bifurcation diagram has no turning points.

The above computations were done using the parametrization of orbits by the parameter  $\alpha$ , and thus the corresponding orbits are inside the region bounded by the homoclinics. This is always the case when  $(-\phi, \phi^*)$  is in this region. When it is outside this region the orbits can still be continued, as explained in Section 3, and the results above still hold using a parametrization of the orbits by either of the parameters introduced therein, namely  $y(-L)$ ,  $z$ , or  $\beta$ .

The results above and the discussion in Section 3 allows us to conclude that the type  $I$  solutions branch continues monotonically to  $T = 0$ , as shown in Figure 7.

**4.2. Behavior of type  $C$  solutions branch.** Consider now solutions of type  $C$ . From (10), the definition of the time maps (5) and (6), and Proposition 1, we conclude that

$$\begin{aligned} T_C(\alpha, \phi) &= 2T(\alpha) + T_1(\alpha, x^*) - T_1(\alpha, \phi) \\ &= T(\alpha) + \underbrace{T_1(\alpha, x^*)}_{>0} + \underbrace{(T(\alpha) - T_1(\alpha, \phi))}_{>0} \\ &> T(\alpha) \\ &> T(\phi) = T^* = 2L^*. \end{aligned}$$

In the other hand, since by (7) and (10) we can write  $T_C(\alpha) = 2T(\alpha) - T_I(\alpha)$ , we conclude that

$$\frac{\partial T_C}{\partial \alpha}(\alpha, \phi) = 2T'(\alpha) - \frac{\partial T_I}{\partial \alpha}(\alpha, \phi) > 0,$$

where the positivity comes from Proposition 1 and the result in Section 4.1. Note that orbits of type  $C$  are always inside the region bounded by the homoclinics and so this analysis is enough to conclude that, like the branch of type  $I$  solutions, the type  $C$  solutions branch do not have turning points and, from Proposition 1.(1), exists globally when  $L \rightarrow +\infty$ , since type  $C$  orbits take progressively longer times as  $\alpha \rightarrow \pi/2..$

**4.3. Local behavior of type  $B$  solutions branch.** In this section we study the behavior of the solution branch of type  $B$  solutions locally close to the bifurcation point.

Consider the branch of bifurcating solutions of (2)–(3) denoted by  $B$  in Section 3. As already observed, the time spent by an orbit of type  $B$  is given by

$$(13) \quad T_B(\alpha, \phi) = T_1(\alpha, \phi) + T_1(\alpha, x^*(\alpha)),$$

where  $T_1$  is the time map defined by (6) and  $x^*$  is defined by (11). Please see the plot of a type  $B$  orbit in Figure 2 in order to clarify this notation.

Since type  $B$  solutions can be continued above the homoclinic orbit to  $(-\frac{\pi}{2}, 0) \equiv (\frac{\pi}{2}, 0)$  in  $\{y > 0\}$  it is natural to consider the orbit parametrized by the ordinate of one of its points. It turns out that, from the computational point of view, an appropriate parameter is the square of the ordinate  $y(-L)$  of the initial point of the orbit. We shall denote this parameter by  $z$ . Using  $V(-\phi, \sqrt{z}) = V(-\alpha, 0)$ , we can obtain the expression for  $T_B$  from (9) when the orbit is bounded by the homoclinics and extended to larger values of  $z$  as explained in Section 2. We thus have

$$(14) \quad T_B(z, \phi) = \int_0^\phi (z - \cos 2\phi + \cos 2x)^{-1/2} dx + \int_0^{\bar{x}^*(z)} (z - \cos 2\phi + \cos 2x)^{-1/2} dx$$

where  $z \in [0, 2]$ ,  $\phi \in (0, \frac{\pi}{2})$ , and  $\bar{x}^*(z)$  is the function  $x^*$  expressed in the new variable  $z$ , defined above in (12).

**4.3.1. Computations of  $\frac{\partial T_B}{\partial z}$ .** We want to prove that for  $z$  sufficiently close to zero the time map satisfies  $T_B(z, \phi) < T_B(0, \phi)$ . To achieve this, we prove, in Proposition 4, that  $\frac{\partial T_B}{\partial z}(0) = -\infty$ , which obviously implies the inequality.

**Proposition 2.**  $\frac{\partial T_B}{\partial z}(z, \phi) \rightarrow -\infty$  as  $z \rightarrow 0$ .

*Proof.* Differentiating (14) with respect to  $z$  we get

$$(15) \quad \begin{aligned} 2 \frac{\partial T_B}{\partial z}(z, \phi) &= - \int_0^\phi (z - \cos 2\phi + \cos 2x)^{-3/2} dx - \\ &\quad - \int_0^{\bar{x}^*(z)} (z - \cos 2\phi + \cos 2x)^{-3/2} dx + \\ &\quad + 2(z - \cos 2\phi + \cos 2\bar{x}^*(z))^{-\frac{1}{2}} \frac{d\bar{x}^*}{dz}(z) \\ &= - \int_0^\phi (z - \cos 2\phi + \cos 2x)^{-3/2} dx - \\ &\quad - \int_0^{\bar{x}^*(z)} (z - \cos 2\phi + \cos 2x)^{-3/2} dx + \\ &\quad + z^{-\frac{1}{2}} (2 - z)^{-\frac{1}{2}} (1 - \cos 2\phi)^{-\frac{1}{2}}. \end{aligned}$$

We now estimate the integral terms in this expression, starting with the second integral. We first need to look at the behavior of  $z \mapsto \bar{x}^*(z)$ : a simple application of the following generalized Taylor expansion

$$(16) \quad \arccos(1-x) = \sqrt{2x} + \frac{(2x)^{\frac{3}{2}}}{24} + O(x^2) \quad \text{as } x \rightarrow 0$$

allows us to write

$$(17) \quad \bar{x}^*(z) = \frac{1}{\sqrt{2}}z^{\frac{1}{2}} + \frac{\sqrt{2}}{24}z^{\frac{3}{2}} + O(z^2), \quad \text{as } z \rightarrow 0.$$

**Lemma 1.**  $\int_0^{\bar{x}^*(z)} (z - \cos 2\phi + \cos 2x)^{-3/2} dx = O(z^{\frac{1}{2}}) \quad \text{as } z \rightarrow 0.$

*Proof.* Since  $1 - \cos 2\phi = z - \cos 2\phi + \cos 2x^*(z) < z - \cos 2\phi + \cos 2x < z + 2$ , and using (17), we get, as  $z \rightarrow 0$ ,

$$\frac{1}{4}z^{\frac{1}{2}} + O(z^{\frac{3}{2}}) < \int_0^{\bar{x}^*(z)} (z - \cos 2\phi + \cos 2x)^{-3/2} dx \leq \frac{1}{\sqrt{2}}(1 - \cos 2\phi)^{-\frac{3}{2}}z^{\frac{1}{2}} + O(z^{\frac{3}{2}}),$$

which proves the lemma.  $\square$

**Lemma 2.**  $\int_0^\phi (z - \cos 2\phi + \cos 2x)^{-3/2} dx = z^{-\frac{1}{2}} \left( \frac{1}{\sin 2\phi} + o(1) \right) \quad \text{as } z \rightarrow 0.$

*Proof.* Consider the trigonometric identity

$$(18) \quad \cos a - \cos b = 2 \sin \frac{b+a}{2} \sin \frac{b-a}{2}$$

and write the integral as

$$\int_0^\phi (z + 2 \sin(\phi+x) \sin(\phi-x))^{-3/2} dx.$$

Considering the change of variable  $x \mapsto t$  defined by  $zt = \sin(\phi-x)$  we have  $\frac{dt}{dx} = -\frac{1}{z}\sqrt{1-(zt)^2}$ , and the integral becomes

$$(19) \quad \begin{aligned} & z^{-\frac{1}{2}} \int_0^{\frac{\sin \phi}{z}} \frac{1}{\sqrt{1-(zt)^2} \left(1 + 2t \sin(2\phi - \arcsin(zt))\right)^{\frac{3}{2}}} dt = \\ & = z^{-\frac{1}{2}} \int_0^{+\infty} \frac{\mathbf{1}_{(0, \frac{\sin \phi}{z})}(t)}{\underbrace{\sqrt{1-(zt)^2} \left(1 + 2t \sin(2\phi - \arcsin(zt))\right)^{\frac{3}{2}}}_{=: f(z,t)}} dt \end{aligned}$$

Observe now that

$$\lim_{z \rightarrow 0} f(z,t) = \frac{1}{(1 + 2t \sin 2\phi)^{\frac{3}{2}}} =: f(t), \quad \text{pointwise in } t,$$

and note also that, since  $0 \leq zt \leq \sin \phi$  and  $0 < \phi < \frac{\pi}{2}$ , we conclude that  $\sin(2\phi - \arcsin(zt))$  is positive and bounded away from zero satisfying<sup>1</sup>  $\sin(2\phi - \arcsin(zt)) >$

<sup>1</sup>Recall the notation  $a \wedge b = \min\{a, b\}$ ,

$\sin 2\phi \wedge \sin \phi =: m(\phi) > 0$ . Also  $\sqrt{1 - (zt)^2} \geq \sqrt{1 - \sin^2 \phi} = \cos \phi > 0$ . From these it follows that

$$\begin{aligned} 0 < f(z, t) &\leq \frac{1}{\cos \phi} \frac{\mathbf{1}_{(0, \frac{\sin \phi}{z})}(t)}{\left(1 + 2tm(\phi)\right)^{\frac{3}{2}}} \\ &\leq \frac{1}{\cos \phi} \frac{1}{\left(1 + 2tm(\phi)\right)^{\frac{3}{2}}} =: g(t) \end{aligned}$$

and  $g$  is integrable in  $[0, +\infty)$ . Hence, by the Lebesgue's dominated convergence theorem applied to the integral in (19) we conclude that, as  $z \rightarrow 0$ ,

$$\int_0^{+\infty} f(z, t) dt = \int_0^{+\infty} \frac{1}{\left(1 + 2t \sin 2\phi\right)^{\frac{3}{2}}} dt + o(1) = \frac{1}{\sin 2\phi} + o(1),$$

and this concludes the proof of the lemma.  $\square$

Collecting the results in the above lemmas we can write, as  $z \rightarrow 0$ ,

$$\begin{aligned} 2 \frac{\partial T_B}{\partial z}(z, \phi) &= -z^{-\frac{1}{2}} \left( \frac{1}{\sin 2\phi} + o(1) \right) + z^{-\frac{1}{2}} \frac{1}{\sqrt{2}} (1 - \cos 2\phi)^{-\frac{1}{2}} + O(z^{\frac{1}{2}}) \\ &= -z^{-\frac{1}{2}} \left( \frac{1}{\sin 2\phi} - \frac{1}{\sqrt{2}(1 - \cos 2\phi)^{\frac{1}{2}}} + o(1) \right) \\ (20) \quad &= -z^{-\frac{1}{2}} \left( \frac{\sqrt{2}(1 - \cos 2\phi)^{\frac{1}{2}} - \sin 2\phi}{\sqrt{2} \sin 2\phi (1 - \cos 2\phi)^{\frac{1}{2}}} + o(1) \right). \end{aligned}$$

Consider the function defined in the interval  $[0, \pi)$  by  $h(x) = 2(1 - \cos x) - \sin^2 x$ . Clearly  $h(0) = 0$  and  $h'(x) > 0$  for  $x \in (0, \pi)$ . Thus  $h(x) > 0$  if  $x \in (0, \pi)$ . This implies that  $2(1 - \cos 2\phi) > \sin^2 2\phi$  for all  $\phi \in (0, \frac{\pi}{2})$  and the monotonicity of  $\sqrt{\cdot}$  entails  $\sqrt{2}(1 - \cos 2\phi)^{\frac{1}{2}} > \sin 2\phi$ . Using this in (20) completes the proof of Proposition 2.  $\square$

The next proposition is an elementary result in Real Analysis that we state and prove for completeness

**Proposition 3.** *Let  $\psi : [0, c) \rightarrow \mathbb{R}$  be a function continuous in  $[0, c)$ , differentiable in  $(0, c)$ , and assume that  $\psi'(x) \rightarrow -\infty$  as  $x \rightarrow 0$ . Then, the following holds true:*

$$\psi'(0) := \lim_{\xi \rightarrow 0^+} \frac{\psi(\xi) - \psi(0)}{\xi} = -\infty.$$

*Proof.* Fix  $\xi \in (0, c)$  and apply the mean value theorem to the interval  $[0, \xi]$ . We conclude that there exists  $x \in (0, \xi)$  such that

$$\frac{\psi(\xi) - \psi(0)}{\xi} = \psi'(x).$$

Passing to the limit as  $\xi \rightarrow 0$  in both sides of this expression, and using the assumption about  $\psi'(x)$  when  $x$  approaches 0 in the right-hand side, we conclude the proof.  $\square$

We can now apply Propositions 2 and 3 to immediately conclude that

**Proposition 4.**  $\frac{\partial T_B}{\partial z}(0, \phi) = -\infty$ .

The results of Propositions 2 and 4 imply that the time taken by a solution of type  $B$  close to the bifurcation point is smaller than the time  $T^*$  taken by the critical solution  $\gamma^*$ .

Actually, for the study of type  $B$  solutions it would have been enough to prove that the derivative  $\frac{\partial T_B}{\partial z}(z, \phi)$  is negative for all  $z \geq 0$  sufficiently small. The fact that it is not just a negative real number is needed for the study of solution branches that correspond to solutions circling the origin  $k$  times, which will be presented in section 5. We will see that there are solutions analogous to those of type  $B$  circling the origin  $k$  times and taking a time given by

$$T_{B_k}(z, \phi) = 4kT(z) + T_B(z, \phi).$$

Since  $T'(0) \in \mathbb{R}^+$ , the fact that  $\frac{\partial T_B}{\partial z}(0, \phi) < 0$  is smaller than any negative real number is what justifies that the bifurcation diagrams for the “ $k$  branches” close to their bifurcation points are qualitatively similar to the case we are presently studying (cf. discussion in section 5; see also Figure 13).

**4.4. On the global behavior of type  $B$  solutions branch.** The result obtained in the previous section for the time taken by a type  $B$  solution is of a local character: it is valid when the type  $B$  orbit is close to the critical one  $\gamma^*$ , i.e., when the value of the parameter indexing the orbit (be it  $\alpha$ ,  $\beta$ , or  $y(-L)$ ) is sufficiently close to the value of the corresponding one in the critical orbit ( $\phi$ ,  $\phi^*$ , or 0, resp.).

From the study presented in Section 3 we concluded that the type  $B$  branch of solutions can be continued away from the neighborhood of the critical orbit, and solutions in this branch, parametrized by the value of  $y(-L)$  only cease to exist when the parameter value is  $y(-L) = \sqrt{2}$ . To understand the global behavior of this branch for  $y(-L) \in (0, \sqrt{2})$  we need to know the behavior of  $y(-L) \mapsto T_B(y(-L))$ . In particular, if we prove that this function is convex, we conclude that the branch of type  $B$  solutions has a unique saddle-node point in the bifurcation diagram.

As in Section 4.3, let us parameterize type  $B$  orbits by  $z = y(-L)^2$ .

Differentiating (15) with respect to  $z$  we get, after some algebraic manipulations,

$$\begin{aligned} 4 \frac{\partial^2 T_B}{\partial z^2}(z, \phi) &= 3 \int_0^\phi (z - \cos 2\phi + \cos 2x)^{-5/2} dx + \\ (21) \quad &+ 3 \int_0^{\bar{x}^*(z)} (z - \cos 2\phi + \cos 2x)^{-5/2} dx + \\ &+ z^{-\frac{3}{2}} (2-z)^{-\frac{3}{2}} (1 - \cos 2\phi)^{-\frac{3}{2}} g(z, \phi), \end{aligned}$$

where

$$(22) \quad g(z, \phi) := z^2 - (2 \cos 2\phi)z - 2(1 - \cos 2\phi).$$

When  $g$  is negative, the sign of  $\frac{\partial^2 T_B}{\partial z^2}(z, \phi)$  depends on the balance between the two positive integrals and the (negative) last term in (21), and its determination seems to be a challenging problem. However, close to the border  $z = 0$  we can compute the sign of  $\frac{\partial^2 T_B}{\partial z^2}$  using the asymptotic technique employed in the proof of Lemma 2:

**Lemma 3.**  $\frac{\partial^2 T_B}{\partial z^2}(z, \phi) > 0$  as  $z \rightarrow 0$ .

*Proof.* From (21) we have

$$(23) \quad 4 \frac{\partial^2 T_B}{\partial z^2}(z, \phi) \geq 3 \int_0^\phi (z - \cos 2\phi + \cos 2x)^{-5/2} dx + z^{-\frac{3}{2}}(2-z)^{-\frac{3}{2}}(1 - \cos 2\phi)^{-\frac{3}{2}} g(z, \phi).$$

Using the trigonometric identity (18) and the change of variable  $x \mapsto t$ , with  $zt = \sin(\phi - x)$ , in the integral in (23), we can write

$$\int_0^\phi (z - \cos 2\phi + \cos 2x)^{-\frac{5}{2}} dx = z^{-\frac{3}{2}} \int_0^{+\infty} \frac{\mathbf{1}_{(0, \frac{\sin \phi}{z})}(t)}{\sqrt{1 - (zt)^2} \left(1 + 2t \sin(2\phi - \arcsin(zt))\right)^{\frac{5}{2}}} dt.$$

Observing that the integral in right-hand side is like (19) with  $-1/2$  changed to  $-3/2$  and  $3/2$  to  $5/2$ , we can apply the argument in the proof of Lemma 2 to obtain, as  $z \rightarrow 0$ ,

$$(24) \quad \int_0^\phi (z - \cos 2\phi + \cos 2x)^{-\frac{5}{2}} dx = z^{-\frac{3}{2}} \int_0^{+\infty} \frac{1}{(1 + 2t \sin 2\phi)^{\frac{5}{2}}} dt + o(1) = \frac{1}{3 \sin 2\phi} + o(1).$$

Now, using the definition of  $g$ , (22), to write  $g(z, \phi) = -2(1 - \cos 2\phi) + O(z)$  as  $z \rightarrow 0$ , observing that  $\sin 2\phi = (1 - \cos^2 2\phi)^{\frac{1}{2}} = (1 - \cos 2\phi)^{\frac{1}{2}}(1 + \cos 2\phi)^{\frac{1}{2}}$ , and substituting (24) into (23), we obtain the following, as  $z \rightarrow 0$ ,

$$(25) \quad 4 \frac{\partial^2 T_B}{\partial z^2}(z, \phi) \geq z^{-\frac{3}{2}} \frac{1}{(1 - \cos 2\phi)^{\frac{1}{2}}} \left( \frac{1}{(1 + \cos 2\phi)^{\frac{1}{2}}} - \frac{1}{\sqrt{2}} + o(1) \right) > 0,$$

where the positivity is due to  $1 + \cos 2\phi \in (0, 2)$ , and hence  $(1 + \cos 2\phi)^{-\frac{1}{2}} > \frac{1}{\sqrt{2}}$ .  $\square$

Since the direct handling of (21) does not seem promising, we tried to approach the problem of the convexity of  $T_B(z, \phi)$  by the method presented in Smoller [6, Chap. 13§D]: to establish the convexity of  $T_B(z, \phi)$  it is sufficient to prove that, if  $(z, \phi) \in (0, 2) \times (0, \frac{\pi}{2})$  is a stationary point of  $z \mapsto T_B(z, \phi)$ , we have

$$(26) \quad \Phi(z, \phi) := 4 \frac{\partial^2 T_B}{\partial z^2} + 2k(z, \phi) \frac{\partial T_B}{\partial z} > 0,$$

for all functions  $k(z, \phi)$ , because at these points the value of the first derivative  $\frac{\partial T_B}{\partial z}$  is zero, by definition. Thus, if we find a function  $k(z, \phi)$  such that (26) holds for all points  $(z, \phi)$ , we conclude that, for each fixed  $\phi$ ,  $\Phi(z, \phi)$  is convex at each of its stationary points, and thus there can exist only one stationary point.

Now, by (15), (21), and (22), choosing

$$(27) \quad k(z, \phi) := -z^{-1}(2-z)^{-1}(1 - \cos 2\phi)^{-1}g(z, \phi)$$

$$(28) \quad = (1 - \cos 2\phi)^{-1} - 2 \frac{z-1}{z(2-z)},$$

we get

$$(29) \quad \Phi(z, \phi) = \left( \int_0^\phi + \int_0^{\bar{x}^*(z)} \right) h^{-5/2} (3 - kh) dx,$$

where

$$(30) \quad h = h(z, \phi, x) := z - \cos 2\phi + \cos 2x.$$

From the definition of  $k$  it follows that  $k < 0$  whenever  $g > 0$  and, from (29), (30), and  $h(z, \phi, x) < h(z, \phi, 0)$ , we easily conclude that  $\Phi(z, \phi) > 0$  in  $\Omega := \{(z, \phi) \in \mathbb{R}^2 \mid 3 - k(z, \phi)h(z, \phi, 0) > 0\}$ . This set  $\Omega$  is illustrated in Figure 5.

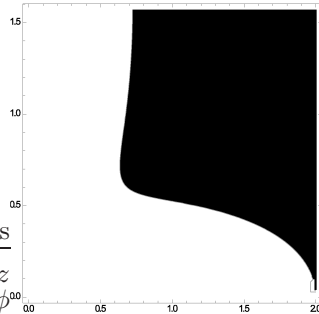


FIGURE 5. Illustration (in black) of the set  $\Omega$  of points  $(z, \phi)$  where  $3 - k(z, \phi)h(z, \phi, 0) > 0$ .

Outside  $\Omega$  the sign of  $\Phi$  is much harder to establish since the two integrals can have opposite signs and be divergent in the boundaries of the domain of  $\Phi$ . Numerical computations using the software Mathematica<sup>©</sup> provide very convincing evidence for the positivity of  $\Phi(z, \phi)$  everywhere in the rectangle  $(0, 2) \times (0, \frac{\pi}{2})$ , as illustrated in Figure 6.

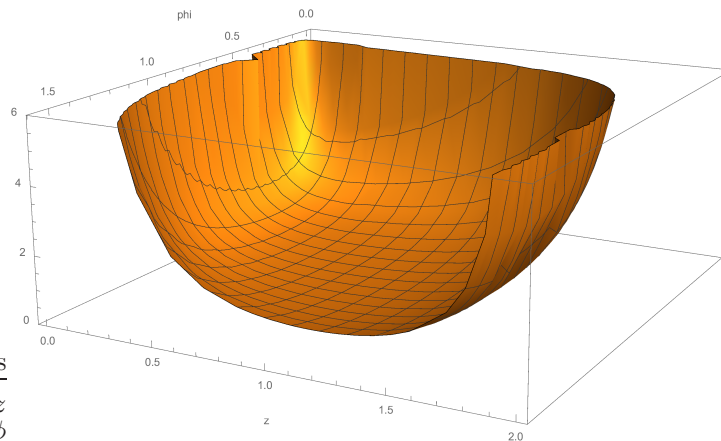


FIGURE 6. Graph of  $(z, \phi) \mapsto \Phi(z, \phi)$

Unfortunately, despite repeated efforts, we were unable to rigorously establish the positivity of  $\Phi$  illustrated in Figure 6, and hence the convexity of  $z \mapsto T_B(z, \phi)$ . Alternative approaches to prove the existence of a single minimum of the graph of  $z \mapsto T_B(z, \phi)$ , based on attempting to define different type of time maps via changes of variables [3, 5] or other analytic approaches [3] were fruitless.

Thus, we state the following

**Conjecture 1.** *For each  $\phi \in (0, \frac{\pi}{2})$ , the function  $z \mapsto T_B(z, \phi)$  is convex.*

For the remainder of this paper we assume this conjecture to hold.

**4.5. Behavior of type  $A$  solutions branch.** From (8) we know that solutions of type  $A$  satisfy  $T_A(\alpha) = 2T(\alpha) - T_B(\alpha)$ . By the results of section 4.3, we know that  $T_B$  is decreasing when  $\alpha > \phi$  close to  $\phi$ , and, by Proposition 1,  $T$  is always increasing. Thus, we conclude that the time  $T_A$  taken by solutions of type  $A$  close to the bifurcation point is larger than the time  $T^*$  taken by the critical solution  $\gamma^*$ .

By putting together all previous (analytical and numerical) results we conclude that the bifurcation diagram of (2)–(3) about  $T^*$  is the one shown in Figure 7.

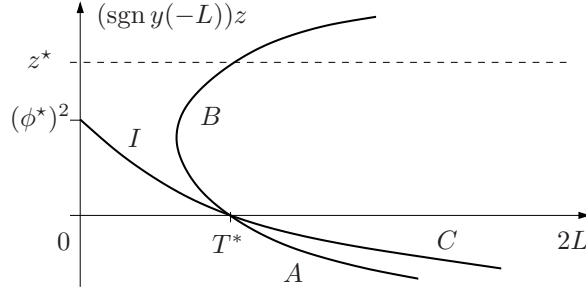


FIGURE 7. Local bifurcation around  $T^* := T(\phi)$ , and global behaviour of the bifurcating branches with  $T < T^*$  assuming the behaviour of  $B$  orbits stated in Conjecture 1. The plotted case corresponds to  $\phi \in (0, \frac{\pi}{4})$ . When  $\phi \in (\frac{\pi}{4}, \frac{\pi}{2})$  the end point of the branch  $I$  occurs above the homoclinic orbit, and thus  $(\phi^*)^2 > z^* := 1 + \cos 2\phi$ .

## 5. OTHER BIFURCATIONS

As was the case of system (2) with non-homogeneous Dirichlet boundary conditions studied in [1, 2], in the present system (2)–(3) with large values of  $L$  we can have solutions turning several times around the origin in the region of the cylindrical phase space bounded by the two homoclinic orbits.

To study these cases we use the same principle of perturbing *critical* orbits  $\gamma_k^*$  defined as  $\gamma^*$  (i.e., satisfying, in addition to (3), homogeneous boundary conditions  $y(-L) = 0$  and  $x(L) = 0$ ) but now turning  $k$  times around the origin. We have also four distinct types of solutions that we can denote by  $I_k$ ,  $A_k$ ,  $B_k$  and  $C_k$ , analogous to  $I$ ,  $A$ ,  $B$  and  $C$ , which can be considered the cases with  $k = 0$  (i.e., orbits that do not have any complete turn around the origin). The time spent by these orbits with  $z$  sufficiently close to zero is obtained by adding  $4kT(\alpha)$  to the times spent by the corresponding  $k = 0$  orbits, e.g.

$$(31) \quad T_{I_k}(z, \phi) = 4kT(z) + T_{I_0}(z, \phi),$$

and likewise for the other types of orbits.

To build a global picture of the  $I_k$  solution branch as  $z$  increases away from  $z = 0$  we need to start by recalling what happens with the  $I$  branch (i.e.: with the case  $k = 0$ ). This was studied in sections 3 and 4.1, and illustrated in figures 3 and 7: the  $I$  branch of solutions collapses to a single point and disappears when  $z = \sqrt{\phi^*}$ .

In the case of  $I_k$  with  $k \geq 1$  an entirely different behaviour takes place: the  $I_k$  branch of solutions exists for all  $z < z^* := 1 + \cos 2\phi$ , where  $z^*$  is the value of  $z$  of the point on the homoclinic orbit with  $x = -\phi$ , and  $T_{I_k}(z) \rightarrow +\infty$  when  $z \rightarrow z^*$ . In fact we have the two situations we now describe:

Suppose  $\phi \in (\frac{\pi}{4}, \frac{\pi}{2})$ , then  $\cos 2\phi < 0$  and thus  $z^* = 1 + \cos 2\phi < 1 - \cos 2\phi = (\phi^*)^2$  which implies that the point where the branch of solutions of type  $I$  collapse,  $P^* = (-\phi, \phi^*)$  in Figure 3, is above the point  $(-\phi, z^*)$  at the homoclinic. This implies that, as  $z \uparrow z^*$ , the orbits of type  $I_k$  converge to the homoclinic net constituted by the point  $(-\frac{\pi}{2}, 0) \equiv (\frac{\pi}{2}, 0)$  and the two homoclinic orbits, as illustrated in Figure 8. The time spent will, obviously, converge to  $+\infty$ .

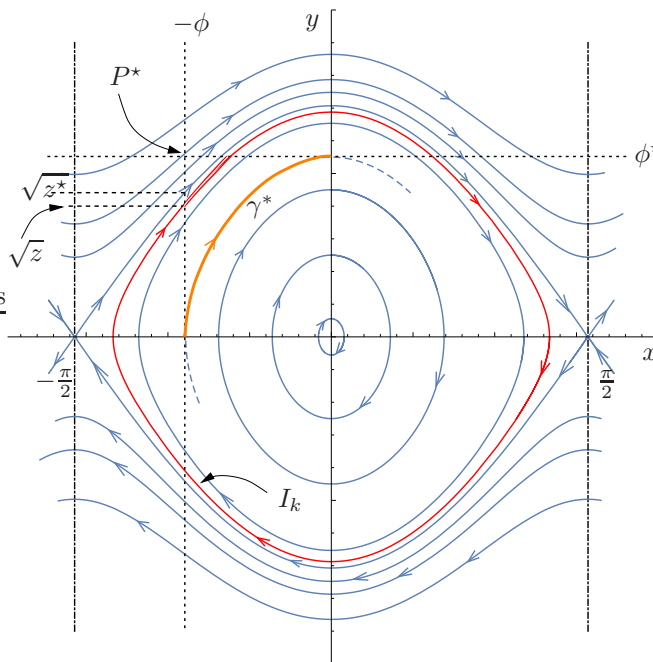


FIGURE 8. An orbit of type  $I_k$ , with  $k = 1$ , and with  $z$  close to  $z^*$ . The case shown corresponds to  $\phi \in (\frac{\pi}{4}, \frac{\pi}{2})$ , in which case  $P^*$  is outside the homoclinic net.

Assume now  $\phi \in (0, \frac{\pi}{4})$ . Then  $\cos 2\phi > 0$  and thus  $z^* = 1 + \cos 2\phi > 1 - \cos 2\phi = (\phi^*)^2$  which implies that the point  $P^*$  is now located inside the homoclinic net, as illustrated in Figure 9. It is clear from this figure that the time spent by these type of orbits  $I_k$  is given by

$$(32) \quad T_{I_k}(z, \phi) = 4kT(z) - T_{I_0}(z, \phi).$$

From Proposition 1, section 4.1, and from  $V(-\alpha, 0) = V(-\phi, \sqrt{z})$ , which results in the relation  $\alpha = \frac{1}{2} \arccos(\cos 2\phi - z)$ , it is easy to conclude that orbits whose time map is given by (32) satisfy

$$(33) \quad \frac{\partial T_{I_k}}{\partial z}(z, \phi) > 0$$

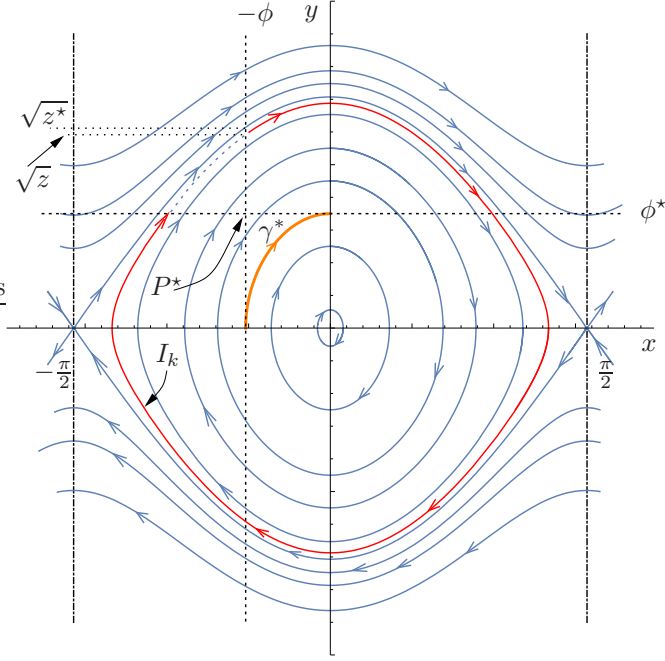


FIGURE 9. An orbit of type  $I_k$ , with  $k = 1$ , and with  $z$  close to  $z^*$ . The case shown corresponds to  $\phi \in (0, \frac{\pi}{4})$ , in which case  $P^*$  is inside the homoclinic net.

and hence the corresponding solution branch in the bifurcation diagram is the graph of a monotonic increasing function converging to the horizontal asymptote  $z = z^*$  as the time  $L$  converges to  $+\infty$ .

In the other hand, for orbits  $I_k$  that do not enclose the point  $P^*$  (i.e., those illustrated in Figure 8), the computation of  $\frac{\partial T_{I_k}}{\partial z}(z, \phi)$  faces exactly the same problems as we confronted in section 4.4 for the global behaviour of solution branch  $B$ .

Actually, we can repeat the arguments in section 4.3 to conclude that  $\frac{\partial T_{I_k}}{\partial z}(z, \phi) \rightarrow -\infty$  as  $z \rightarrow 0$ . Since, as we noted above,  $T_{I_k}(z, \phi) \rightarrow +\infty$  as  $z \rightarrow z^*$ , we conclude that the  $T_{I_k}(z, \phi)$  must have at least one minimum for some<sup>2</sup>  $z \in (0, \phi^*)$ . A numerical study entirely analogous the one presented in section 4.4 allows us to believe that Conjecture 1 is also valid for the branches  $I_k$  with  $k \geq 1$ .

From the fact that the time maps for the branches  $B_k$  with  $k \geq 1$  are, like in (31), obtained from the one of branch  $B$  by adding  $4kT(z)$ , the conclusion we reached for the branches  $I_k$  is repeated for the  $B_k$ s.

Thus, from the discussion above and assuming Conjecture 1 holds true for the branches  $I_k$  and  $B_k$  with  $k \geq 1$ , the bifurcation scheme for the solution branches with  $k \geq 1$  is shown in Figure 10.

<sup>2</sup>Observe that, due to (33), if the interval  $(\phi^*, z^*)$  is not empty the piece of the solution branch  $I_k$  with  $z$  in this interval is monotonic and so the minima of the  $I_k$  branch must necessarily correspond to values  $z < \phi^*$ .

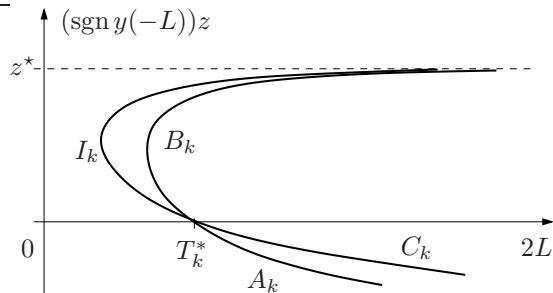


FIGURE 10. Bifurcating branches  $I_k$ ,  $A_k$ ,  $B_k$  and  $C_k$ , with  $k \geq 1$ , assuming the behaviour of the branch  $B_0$  stated in Conjecture 1 is also valid for branches  $I_k$  and  $B_k$ . Here  $T_k^* := 4kT(\phi)$ .

Additional to these orbits, there are another two families of orbits, that we denote by  $D_k$  and  $D'_k$ , which correspond to orbits analogous to  $B$  and  $B'$  but are located above the homoclinic orbit with positive  $y$ -component, and turn around the cylindrical phase space  $k$  times (see example in Figure 11).

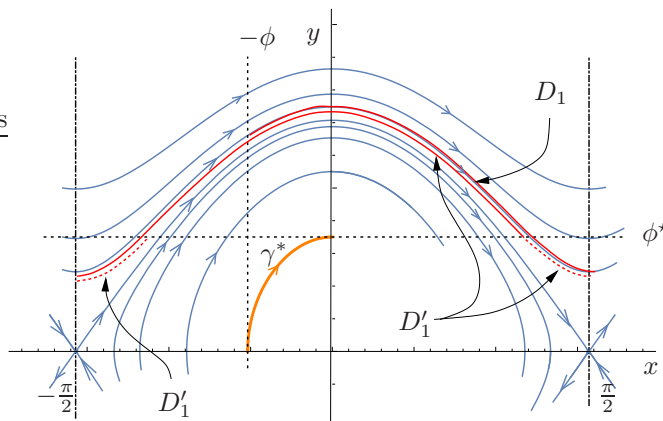


FIGURE 11. Orbits of type  $D_k$  and  $D'_k$ , with  $k = 1$ . The orbit  $D'_1$  is represented by the full line (dashed and undashed);  $D_1$  is represented by the undashed part only. In this plot each time the orbit  $D_1$  or  $D'_1$  passes through a same point the line is slightly deflected in order to facilitate the reading.

The amount of time spent by these orbits are given by

$$(34) \quad T_{D_k}(z, \phi) := 2kT_1(z, \frac{\pi}{2}) + T_1(z, \phi) + T_1(z, \bar{x}^*(z))$$

$$(35) \quad T_{D'_k}(z, \phi) := 2(k+1)T_1(z, \frac{\pi}{2}) + T_1(z, \phi) - T_1(z, \bar{x}^*(z)),$$

where, for each  $\phi \in (0, \frac{\pi}{2})$ ,  $z$  varies from  $z^* := 1 + \cos 2\phi$ , the value of ordinate square of the point of intersection of  $x = -\phi$  and the homoclinic orbit, obtained from  $V(-\frac{\pi}{2}, 0) = V(-\phi, \sqrt{z^*})$ , and 2, the biggest value of  $z$  for which the orbit intersects the line  $y = \phi^*$ .

We can see directly from Figure 11 that when  $z = 2$  the end points of  $D_k$  and  $D'_k$  are the same (and coincide with the point  $(\frac{\pi}{2}, \phi^*)$ .) This can also be obtained from (34)-(35):

$$\begin{aligned}
T_{D'_k}(z, \phi) &= 2(k+1)T_1(z, \frac{\pi}{2}) + T_1(z, \phi) - T_1(z, \bar{x}^*(z)) \\
&= T_{D_k}(z, \phi) + 2(T_1(z, \frac{\pi}{2}) - T_1(z, \bar{x}^*(z))) \\
(36) \qquad \qquad &\geq T_{D_k}(z, \phi),
\end{aligned}$$

since, from its definition,  $T_1(z, \cdot)$  is monotonic increasing, and, by (12),  $\bar{x}^*(z) \leq \frac{\pi}{2}$  with equality only when  $z = 2$ , because  $\bar{x}^*(2) = \frac{1}{2} \arccos(-1) = \frac{\pi}{2}$ .

From (36) we conclude that, for each  $k$ , the branches  $D_k$  and  $D'_k$  exist for all  $z \in (z^*, 2)$  and, in a bifurcation diagram with time as the bifurcation variable and  $z$  as the dependent variable, the  $D_k$  branch will always be to the left of the  $D'_k$ , except at one single point, with ordinate  $z = 2$ , where they coincide.

To study the monotonicity of the branches  $D_k$  and  $D'_k$  we again use the time maps (34) and (35), respectively. The last is easier: differentiating (35) with respect to  $z$  we obtain, after some algebraic manipulations,

$$\begin{aligned}
\frac{\partial T_{D'_k}}{\partial z}(z, \phi) &= -(k + \frac{1}{2}) \int_0^{\frac{\pi}{2}} (z - \cos 2\phi + \cos 2x)^{-3/2} dx \\
&\quad - \frac{1}{2} \int_0^{\phi} (z - \cos 2\phi + \cos 2x)^{-3/2} dx \\
&\quad - \frac{1}{2} \int_{\bar{x}^*(z)}^{\frac{\pi}{2}} (z - \cos 2\phi + \cos 2x)^{-3/2} dx \\
&\quad - \frac{1}{2} z^{-\frac{1}{2}} (2-z)^{-\frac{1}{2}} (1 - \cos 2\phi)^{-\frac{1}{2}} \\
(37) \qquad \qquad &< 0,
\end{aligned}$$

and  $\frac{\partial T_{D'_k}}{\partial z} \rightarrow -\infty$  when  $z \rightarrow z^*$  and when  $z \rightarrow 2$ .

The same computation for the branch  $D_k$  runs into the difficulties already encountered before when studying the branches  $B_k$  (with  $k \geq 0$ ) and  $I_k$  (with  $k \geq 1$ ). The expression for the derivative of the time map is

$$\begin{aligned}
\frac{\partial T_{D_k}}{\partial z}(z, \phi) &= -(k+1) \int_0^{\frac{\pi}{2}} (z - \cos 2\phi + \cos 2x)^{-3/2} dx \\
&\quad - \frac{1}{2} \int_0^{\phi} (z - \cos 2\phi + \cos 2x)^{-3/2} dx \\
&\quad - \frac{1}{2} \int_0^{\bar{x}^*(z)} (z - \cos 2\phi + \cos 2x)^{-3/2} dx \\
(38) \qquad \qquad &+ \frac{1}{2} z^{-\frac{1}{2}} (2-z)^{-\frac{1}{2}} (1 - \cos 2\phi)^{-\frac{1}{2}},
\end{aligned}$$

and  $\frac{\partial T_{D_k}}{\partial z} \rightarrow -\infty$  when  $z \rightarrow z^*$ , and  $\frac{\partial T_{D_k}}{\partial z} \rightarrow +\infty$  when  $z \rightarrow 2$ . The existence of a unique minimum of  $T_{D_k}(\cdot, \phi)$  can be checked numerically like was done in the case of the  $B$  branch in section 4.4, but, as there, the rigorous proof eludes us at present. All numerical evidence points to the validity of Conjecture 1 also for the function  $z \mapsto T_{D_k}(z, \phi)$ , and assuming this the situation with branches  $D_k$  and  $D'_k$  is illustrated in Figure 12.

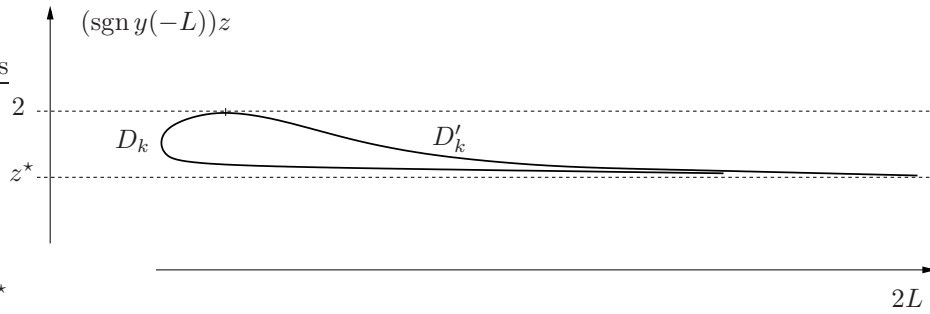


FIGURE 12. Solution branches  $D_k$  and  $D'_k$ , with  $k \geq 1$ , assuming that the behaviour of branch  $B$  stated in Conjecture 1 is also valid for branches  $D_k$ .

## 6. CONCLUSION

Gathering the results and discussions from the previous sections we can construct the following schematic bifurcation diagram for solutions of (2)–(3).

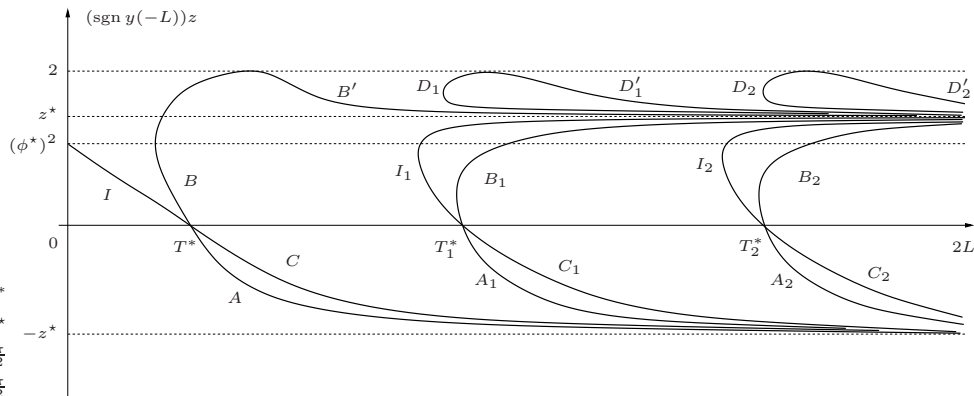


FIGURE 13. Schematic bifurcation diagram for system (2)–(3) with  $\phi \in (0, \frac{\pi}{4})$ , assuming validity of Conjecture 1 for the relevant branches, as explained in the text. For the notation used in this figure see the text.

## ACKNOWLEDGEMENTS

FPdC and JTP were partially funded by FCT/Portugal through project RD0447/CAMGSD/2015. FPdC acknowledges financial support provided by the University of Strathclyde David Anderson Research Professorship. Parts of sections 3, 4.1, and 4.2 first appeared in the dissertation submitted by KX to the National University of Laos, Vientiane, Laos, in July 2017, as part of the requirements for the degree of MSc in Applied Mathematics.

## REFERENCES

- [1] F.P. da Costa, E.C. Gartland, Jr., M. Grinfeld, J.T. Pinto, Bifurcation analysis of the twist-Fréedericksz transition in a nematic liquid-crystal cell with pre-twist boundary conditions; *Euro. J. Appl. Math.*, **20** (2009) 269–287.
- [2] F.P. da Costa, M.I. Méndez, J.T. Pinto, Bifurcation analysis of the twist-Fréedericksz transition in a nematic liquid-crystal cell with pre-twist boundary conditions: the asymmetric case; *Euro. J. Appl. Math.*, **28** (2017) 243–260.
- [3] P. Korman, *Global Solution Curves for Semilinear Elliptic Equations*, World Scientific, Singapore, 2012.
- [4] N. Mottram, private communication, 2018.
- [5] R. Schaaf, *Global Solution Branches of Two Point Boundary Value Problems*, Lecture Notes in Mathematics, vol. 1458, Springer-Verlag, Berlin, Heidelberg, 1990.
- [6] J. Smoller, *Shock Waves and Reaction-Diffusion Equations*, 2nd Ed., Grundlehren der mathematischen Wissenschaften 258, Springer, New York, 1994.

DEPARTAMENTO DE CIÊNCIAS E TECNOLOGIA, UNIVERSIDADE ABERTA, LISBOA, PORTUGAL, AND  
CENTRE FOR MATHEMATICAL ANALYSIS, GEOMETRY, AND DYNAMICAL SYSTEMS, INSTITUTO SUPERIOR  
TÉCNICO, UNIVERSIDADE DE LISBOA, LISBOA, PORTUGAL

*E-mail address:* `fcosta@uab.pt`

DEPARTMENT OF MATHEMATICS AND STATISTICS, UNIVERSITY OF STRATHCLYDE, GLASGOW,  
UNITED KINGDOM

*E-mail address:* `m.grinfeld@strath.ac.uk`

DEPARTAMENTO DE MATEMÁTICA, INSTITUTO SUPERIOR TÉCNICO, UNIVERSIDADE DE LISBOA,  
LISBOA, PORTUGAL, AND CENTRE FOR MATHEMATICAL ANALYSIS, GEOMETRY, AND DYNAMICAL  
SYSTEMS, INSTITUTO SUPERIOR TÉCNICO, UNIVERSIDADE DE LISBOA, LISBOA, PORTUGAL

*E-mail address:* `jpinto@math.tecnico.ulisboa.pt`

DEPARTMENT OF MATHEMATICS, FACULTY OF NATURAL SCIENCES, NATIONAL UNIVERSITY OF  
LAOS, DONGDOK CAMPUS, VIENTIANE, LAOS

*E-mail address:* `kedtysack@gmail.com`